



## Evaluation of Zinc Chelation Ability for Non-Hydroxamic Organic Moieties

Ayad A. Al-Hamashi\*, Shayma L. Abdulhadi, Rusul Mohammed Hasan Ali  
 Department of Pharmaceutical Chemistry, College of Pharmacy, University of Baghdad, Baghdad, Iraq



### Abstract

Histone deacetylase (HDAC) enzymes are zinc-dependent metalloproteinases that are deregulated in a number of diseases, including cancer. The majority of the clinically used HDAC inhibitors are hydroxamates. Limitations in their clinical use due to poor selectivity, pharmacokinetics, and toxic side effects warrant the development of new inhibitors with non-hydroxamate zinc-binding groups (ZBG). Thus, in this work computational and chemical techniques were employed to assess the zinc ion chelation activity for a number of organic moieties that have potential chelation ability. Molecular modeling studies including molecular docking, molecular dynamic simulation, and ADMET experiments were conducted to evaluate the potential chelation activity of the selected organic moieties into HDAC proteins. The chosen moieties were reacted with zinc ion to explore the chelation inclination, and the resulting complexes were characterized using infrared and UV/Vis spectroscopy. According to all findings, the antipyrine (compound **1**) showed a superior *in silico* binding data. The modeling results were supported by the experimental zinc ion chelation tendency.

**Keywords:** histone deacetylase enzymes; zinc-binding groups; molecular docking; molecular dynamic simulation.

### 1. Introduction

Zinc ion is found abundantly in the human body and has a crucial role in several physiological activities including, cell proliferation, differentiation, and apoptosis [1]. It is acting as a cofactor for different types of enzymes through the coordination to amino acid residues that lining the binding site of zinc-dependent enzymes [2]. Histone deacetylase (HDAC) enzymes are an example of zinc-dependent metalloproteins [3]. HDACs have been linked to several diseases, such as neurodegenerative diseases [4], infections [5], human immunodeficiency virus (HIV) [6], cardiac diseases [7], and tumors [8]. Four HDAC inhibitors have been FDA approved for the treatment of cancer (Figure 1a). To date, there are 18 HDAC isoforms. These isoforms are classified into four classes as: class I which includes HDAC1, 2, 3, and 8; class II which includes HDAC 4–7, 9, and 10; class IV which includes HDAC 11; and class III enzymes (Sirt1–7). Classes I, II, and IV are zinc-dependent enzymes, whereas class III is nicotinamide adenine dinucleotide (NADP)-dependent enzymes. The typical HDAC inhibitor is consist of three

essential parts known as zinc-binding group (ZBG), cap group, and linker that connects the two components. The binding of ZBGs to the HDAC zinc ion and the active site surrounding residues is essential for the inhibitory activity and the selectivity of HDAC inhibitors, while the cap group and the linker are mostly manipulating the inhibition selectivity [9]. Modifications in the structure of the ZBGs are an efficient strategy for the creation of new HDAC inhibitors with an optimum potency and selectivity profile [10].

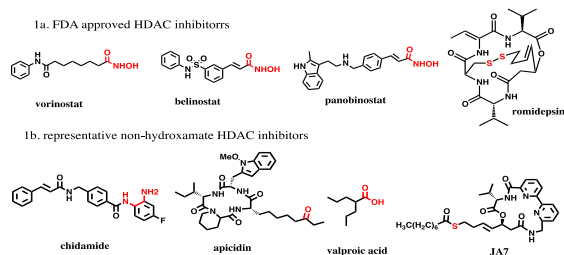


Fig. 1. Selected HDAC inhibitors. (1a) The FDA approved HDAC inhibitors; (1b) Representative non-hydroxamate HDAC inhibitors. The zinc chelating moieties are highlighted in red.

\*Corresponding author e-mail: [a.alhamashi@copharm.uobaghdad.edu.iq](mailto:a.alhamashi@copharm.uobaghdad.edu.iq); (Ayad A. Al-Hamashi).

Receive Date: 01 July 2022, Revise Date: 17 August 2022, Accept Date: 26 August 2022.

DOI: [10.21608/ejchem.2022.147377.6415](https://doi.org/10.21608/ejchem.2022.147377.6415)

©2023 National Information and Documentation Center (NIDOC).

Hydroxamates HDAC inhibitors are the most extensively investigated HDAC inhibitors. Three of the four FDA-approved HDAC inhibitors are involving hydroxamates as ZBG. However, hydroxamate HDAC inhibitors have limited clinical uses due to their poor selectivity and inferior pharmacokinetic properties [11,12]. The non-hydroxamic HDAC inhibitors are widely investigated [10]. The replacing of hydroxamate moiety with benzamides (chidamide) [13], ketones (apicidin) [14], carboxylic acids (valproic acid) [15], or thiols (JA7) [16] (Figure 1b) showed a promising selectivity and potency profile. Therefore, the development of HDAC inhibitors containing new ZBG is highly recommended [17,18]. The adoption of the metal-binding heterocycle isosteres strategy to develop new metalloenzyme inhibitors represents an important strategy to produce selective and biologically active inhibitors [19]. Numerous instants of computer-aided analysis and design of novel inhibitors were noticed recently [20-26]. Hence, in this study molecular modeling studies were carried out to estimate the zinc chelation activity for the selected non-hydroxamate functionalities on HDAC proteins (Figure 2). In addition, the experimental zinc ion chelation tendency was detected by monitoring the spectral changes of the possible zinc chelating moieties.

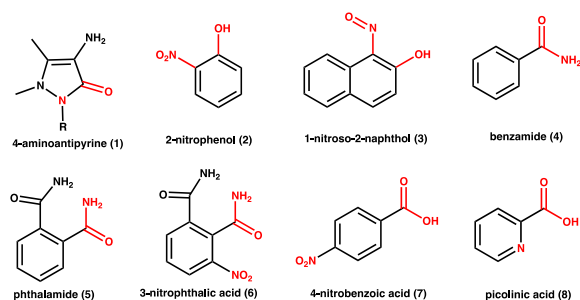


Fig. 2. The chemical structure for the selected fragments as ZBG. The possible zinc chelating atoms are depicted in red.

## 2. Experimental

### 2.1. Material and Instrumentation

All chemicals and solvents were obtained from commercial sources and used without further purification. Antipyrine and zinc chloride were purchased from Sigma-Aldrich, Germany; ethanol purchased from Scharlau, Spain. IR spectra were carried out on Shimadzu FTIR IRAffinity-1 model, Japan. The UV experiments were conducted via UV-Visible spectrophotometer, Cary 100 Conc model, Agilent Technologies, USA. The molecular docking studies were performed utilizing a licensed Schrodinger suite of Glide, Desmond, and Qikprop applications. All the aforementioned instruments were available in the Department of Pharmaceutical

Chemistry, College of Pharmacy, University of Baghdad.

### 2.2. Molecular Docking

The molecular docking studies were performed using Glide tool in the Maestro platform 13.0.135, 2021-4 of Schrodinger suite, LLC, New York, NY, 2021 to assess the binding affinity of the hypothesized ZBGs into the binding site of HDAC2 and HDAC6 enzymes [27]. The Ligprep module was utilized to build the chemical structure of the proposed fragments. The crystal structure for HDAC2 (pdb code: 4LXZ) and HDAC6 (pdb code: 5EDU) proteins were downloaded from Protein Data Bank and prepared through the employing of the protein preparation tool [28]. The protein energy was minimized using OPLS\_2005 force field [29]. The grid box was prepared as  $20 \text{ \AA} \times 20 \text{ \AA} \times 20 \text{ \AA}$ . The flexible ligand docking was implicated under OPLS\_2005 force field. A standard precision docking mode was exploited to generate 10 pose per ligand.

### 2.3. Molecular Dynamic Simulation

The interaction stability between the zinc chelator moieties and HDAC enzymes was investigated using Desmond module of Schrodinger suite, New York, NY, 2021 at 100 ns time period [30]. The proteins were downloaded, and SPC water solvent model was selected. An orthorhombic water boundary box was chosen, and the volume was minimized. The system was neutralized with Cl and Na ions, and default values were selected for the rest of software parameters to build the system. The simulation was run using OPLS3e force field and 1000 frames were recorded. We used the Root Mean Square Deviation (RMSD) to calculate the average change in displacement of a group of atoms for a particular frame compared to a reference frame. In addition, Ligand Root Mean Square Fluctuation (L-RMSF) was measured to characterize the variations in the sites of ligand atoms.

### 2.4. ADMET Profile

The QikProp application Schrodinger, New York, NY, 2021 was used to evaluate the ADMET properties (absorption, distribution, metabolism, excretion, and toxicity) of the designed ligands. To forecast the drug-likeness properties of the suggested molecules, the following information were studied: MW (molecular weight); SASA (solvent accessible surface area); donorHB (number of hydrogen-bond donors); acceptorHB (number of hydrogen-bond acceptors); QPlogHERG (Predicted IC<sub>50</sub> value for blockage of HERG K<sup>+</sup> channel); QPPCaco (predicted apparent Caco-2 cell permeability); QPlogBB (predicted brain/blood partition coefficient); #metab (number of

likely metabolic reactions); QPlogKhsa (prediction of binding to human serum albumin); %oralAbs (predicted qualitative human oral absorption); PSA (Van der Waals surface area of polar nitrogen and oxygen atom).

### 2.5. The General Procedure for Experimental Zinc Complexation

The zinc complexation was carried out through the mixing of 0.01 M of the ZBG organic moieties and 0.01 M of zinc chloride in ethanol. The mixture was refluxed for 4 h and then stirred at room temperature overnight. The mixture was filtered and washed to get fine crystals [31]. Characterization of the formed complexes was performed using UV and FTIR spectroscopy.

## Results and Discussion

### 3.1. Molecular Docking

To evaluate the *in silico* zinc chelation of selected organic moieties on variant HDAC isoforms, the selected moieties were connected into the linker

and the cap group of vorinostat docked into HDAC2 and HDAC6 utilizing Glide software. Compounds showed variant zinc chelation ability as shown in table 1. Compounds **1**, **4**, and **8** demonstrated a relatively higher affinity than vorinostat for both HDAC2 and HDAC6, while compounds **3** and **7** were chelated zinc ion with less affinity. Compound **2** is more selective for HDAC6, while compound **6** is virtually prefers HDAC2. Contrarily, compound **5** does not chelate HDAC2 and HDAC6. Interestingly, the modified antipyrine (compound **1**) displayed a superior virtual binding affinity and high docking score. The modified heterocyclic ring of compound **1** interacting with zinc ion inside the active site residues of both HDAC2 and HDAC6. The interaction is attributed to the bidentate chelation of N2 atom and C3 hydroxyl group of compound **1** with zinc ion. This association facilitated a nice positioning of compound **1** linker inside HDAC2 and HDAC6 active site channel and props the phenyl cap group into outer rim (Figure 3). As a consequence, compound **1** was selected for additional modeling studies for further evaluation.

Table 1. Docking scores of the selected moieties on HDAC2 and HDAC6

Moiety X	HDAC2		HDAC6	
	Zinc chelation	Docking score (Kcal/mol)	Zinc chelation	Docking score (Kcal/mol)
Vorinostat	+	-5.77	+	-5.23
4 amino antipyrine (1)	+	-6.61	+	-7.38
2-nitrophenol (2)	+	-3.73	-	-5.98
1 nitroso 2 naphthol (3)	+	-2.455	+	-3.79
benzamide (4)	+	-7.55	+	-7.78
phthalamide (5)	-	-4.60	-	-4.00
3-nitrophthalic acid (6)	-	-5.87	+	-3.82
4 nitrobenzoic acid (7)	+	-6.09	+	-4.87
picolinic acid (8)	+	-5.69	+	-5.45

### 3.2. Molecular Dynamic Simulation

The molecular dynamic (MD) simulation study was conducted to validate the binding stability between the top-ranked chelator, of compound **1** with HDAC2 and HDAC6. The findings indicated that N2 atom and C3 hydroxyl group of compound **1** are forming a permanent bidentate interaction of 100% with zinc ion and the Asp:Asp:His triad for both HDAC2 and HDAC6. The HDAC2 H145 residue had 86% prevalence of  $\pi$ - $\pi$  association with the antipyrine ring, compared to 44% for HDAC6 H651 residue. In addition, the G305 residue of HDAC2 is forming a stable connection of 94% and 89% with C3 hydroxyl and C4 amine groups, respectively. For HDAC6, the hydrogen bond between residue H610 and C3

hydroxyl is highly stable of 83% probability (Figure 4A and 4B). The predicted stable interaction of the antipyrine-containing molecule with HDAC2 and HDAC6 might indicate a highly promising inhibition activity of antipyrine-containing molecules on HDAC enzymes. The calculated HDAC2-antipyrine RMSD were 0.8-7.2 °Å for ligand and 1.2-2.25 °Å for HDAC2. While the HDAC6-antipyrine RMSD is 4-13.5 °Å for ligand and 1-4.8 °Å for HDAC6 (Figure 4C and 4D). The RMSF data indicated that all atoms of antipyrine ring are essential for the zinc chelation activity for both HDAC2 and HDAC6 (Figure 4E and 4F).

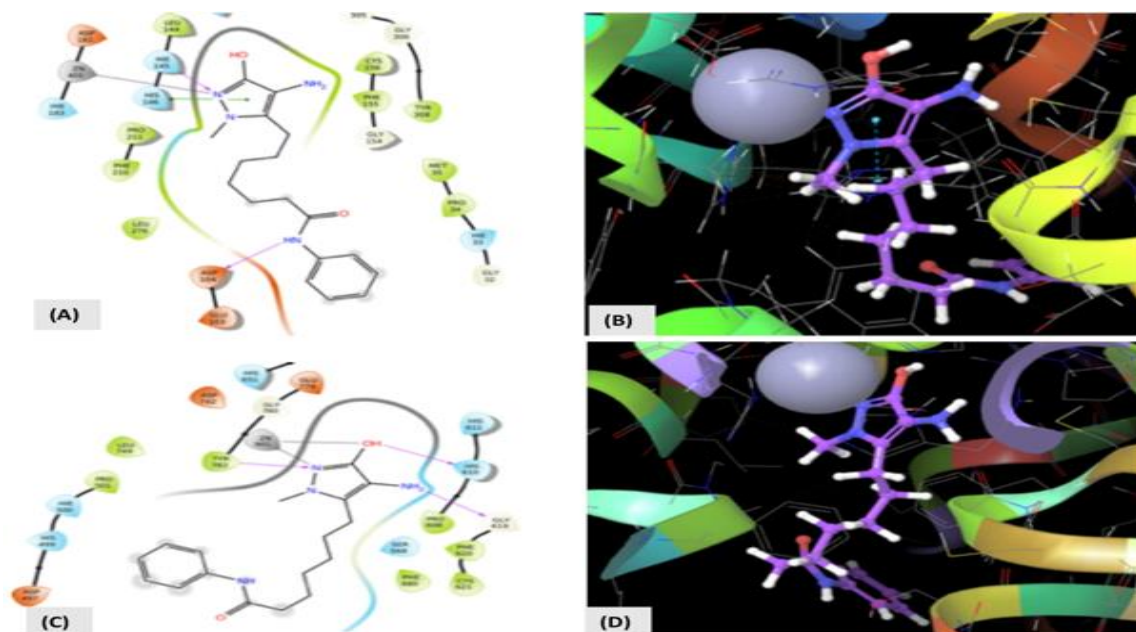


Fig. 3. The molecular docking results of compound 1. (A) 2D interaction of compound 1 with HDAC2 binding site, (B) 3D interaction of compound 1 inside the active site of HDAC2, (C) 2D interaction of compound 1 with HDAC6 binding site, (D) 3D interaction of compound 1 inside the active site of HDAC6.

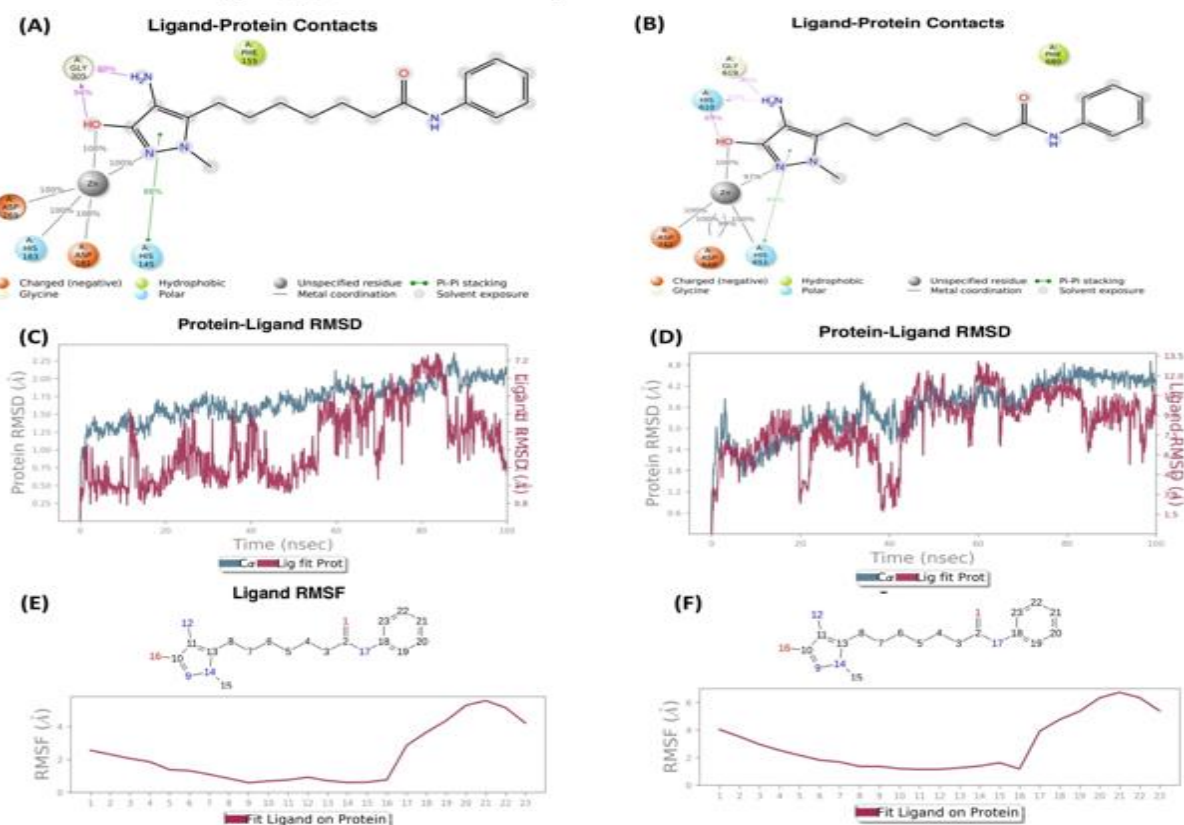


Fig. 4. The molecular dynamic (MD) results for the interaction of compound 1. (A) The MD simulation interaction with HDAC2, (B) The HDAC2-compound 1 RMSD ranges, (C) Compound 1 RMSF with HDAC2, (D) The MD simulation interaction with HDAC6, (E) The HDAC6-compound 1 RMSD ranges, (F) Compound 1 RMSF with HDAC6.

### 3.2. ADMET Profile

To explore the pharmacokinetic features of the docked molecules, virtual ADMET properties were studied using Qikprop software of Schrodinger suite. The results showed that all compounds were not violating the rule of five with an adequate expected

oral absorption. As multiple positions are labile for metabolism, SAR optimization might be needed to increase the metabolic stability (Table 2). Overall, some of these compounds involve fundamental structural features to serve as models for further structural optimization.

Table 2. Virtual ADMET data. MW: molecular weight; SASA solvent accessible surface area; donaorHB: number of hydrogen-bond donors; accprHP: number of hydrogen-bond acceptors; QPlogHERG: Predicted IC50 value for blockage of HERG K+ channel; QPPCaco Predicted apparent Caco-2 cell permeability; QPlogBB: Predicted brain/blood partition coefficient; #metab: Number of likely metabolic reactions; QPlogKhsa: Prediction of binding to human serum albumin; %oralAbs: Predicted qualitative human oral absorption; PSA: Van der Waals surface area of polar nitrogen and oxygen atom.

code	MW	SASA	volume	donorHB	acceptorHB	QPlogHERG	QPlogPCaco	QPlogBB	#metab	QPlogKhsa	%oralAbs	PSA	Rule of 5
SAHA	264	582	964	3	6.7	-4.2	161	-1.6	3	0.76	71	99	0
1	634	657	1119	3.5	4.5	-6.6	62	-1.4	5	0.14	74	102	0
2	237	701	1186	2	4.25	-6.7	175	-2.1	5	0.50	89	101	0
3	632	746	1289	2	4.75	-7.1	394	-1.7	4	0.68	100	87	0
4	436	698	1182	3	5	-6.8	318	-1.7	4	0.31	92	89	0
5	741	740	1266	5	7.5	-6.7	48	-2.8	5	0.07	69	137	0
6	437	755	1305	3	7.5	-3.0	1.1	-3.4	4	0.19	47	167	0
7	032	714	1229	2	5.5	-4.7	18	-2.5	4	0.23	72	126	0
8	680	680	1153	2	5.5	-4.7	2	-1.8	4	0.07	80	98	0

### 3.3. Zinc Complexation

The zinc complexation was chemically deduced through the complexation of the selected moieties with zinc ion. The generated complexes were characterized through the evaluation of the potential chelating moieties via UV and IR spectra. Compared to the free 4-amino antipyrine (compound **1**), the resultant 4-amino antipyrine-zinc ion complex showed a modest shifting to higher UV  $\lambda_{max}$  (Figure 5a). As well as, the IR NH<sub>2</sub> stretching becomes broader and the carbonyl stretching is slightly shifted (Figure 5b). The possible complexation between zinc ion with antipyrine amine and carbonyl moieties might be the reason behind these findings. Therefore,

the possible zinc complexation would support our hypothesis of discovering new ZBG for HDAC inhibition.

## 4. Conclusions

The zinc ion chelation tendency for several organic moieties with HDAC enzymes was assessed through the molecular modeling studies. The *in silico* data were validated with a preliminary experimental zinc ion chelation investigation. The selected moieties exhibited variant binding affinity to HDAC enzymes. Interestingly, the antipyrine pharmacophore demonstrated a superior *in silico* and experimental

chelation tendency. The virtual affinity of compound **1** with HDAC2 and HDAC6 is relatively high. Most likely that the electron-rich moieties of the N2 and C3 hydroxyl groups and the aromatic properties of antipyrine are responsible for the chelation tendency for compound **1**. The molecular dynamic simulation results indicated that the antipyrine ring is generating potent and stable bidentate chelation with zinc ion and the Asp:Asp:His triad residues inside the HDAC

pocket. In conclusion, the antipyrine moiety might represent a potential pharmacophore for developing a future HDAC inhibitor candidate. The inhibition activity, selectivity, and pharmacokinetic properties for compound **1** could be improved through the optimization of the structural features of the linker and the cap group. The synthesis of a library of compound **1** analogs and the evaluation of their biological activity is our future goal.

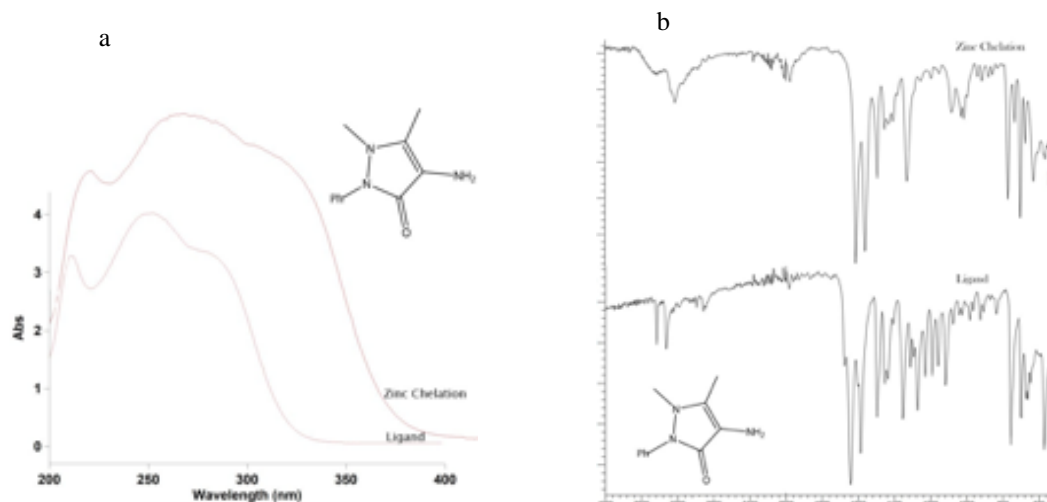


Fig. 5. The comparison of zinc chelated and non-chelated of 4-aminoantipyrine using (a) UV spectrum, (b) IR spectrum.

## 5. Conflicts of interest

There are no conflicts to declare.

## 6. References

- [1] Maret, W.; Sandstead, H.H. Zinc requirements and the risks and benefits of zinc supplementation. *J. Trace Elem. Med. Biol.* **20**, 3–18 (2006).
- [2] Rao B. Recent Developments in the Design of Specific Matrix Metalloproteinase Inhibitors aided by Structural and Computational Studies. *Curr Pharm Des.* **11**(3):295–322 (2005).
- [3] Foglietti C, Filocamo G, Cundari E, et al. Dissecting the biological functions of Drosophila histone deacetylases by RNA interference and transcriptional profiling. *J Biol Chem*, **281**:17968–76 (2006).
- [4] Soragni E, Xu C, Cooper A, et al. Evaluation of histone deacetylase inhibitors as therapeutics for neurodegenerative diseases. *Method Mol Biol*, **793**:495–508 (2011).
- [5] Roger T, Lugin J, Le Roy D, et al. Histone deacetylase inhibitors impair innate immune responses to Toll-like receptor agonists and to infection. *Blood*, **117**:1205–17(2011).
- [6] Saiyed ZM, Gandhi N, Agudelo M, et al. HIV-1 Tat upregulates expression of histone deacetylase-2 (HDAC2) in human neurons: implication for HIV-associated neurocognitive disorder (HAND). *Neurochem Int*; **58**:656–64 (2011).
- [7] Gallo P, Latronico MV, Gallo P, et al. Inhibition of class I histone deacetylase with an apicidin derivative prevents cardiac hypertrophy and failure. *Cardiovasc Res*; **80**:416–24 (2008).
- [8] Marks PA, Rifkind RA, Richon VM, et al. Histone deacetylases and cancer causes and therapies. *Nat Rev Cancer*; **1**:194–202 (2001).
- [9] Manal M, Chandrasekar MJN, Priya JG, Nanjan MJ. Inhibitors of histone deacetylase as antitumor agents: a critical review. *Bioorg Chem*; **67**:18–42 (2016).
- [10] Frühauf, A.; Meyer-Almes, F.-J. Non-Hydroxamate Zinc-Binding Groups as Warheads for Histone Deacetylases. *Molecules*, **26**, 5151(2021).
- [11] Benedetti R, Conte M, Altucci L. Targeting histone deacetylases in diseases: where are we? *Antioxid Redox Signal*; **23**:99–126 (2015).

- [12] Kazantsev AG, Thompson LM. Therapeutic application of histone deacetylase inhibitors for central nervous system disorders. *Nat Rev Drug Discov*; **7**:854–68 (2008).
- [13] Xianping Lu, Zhiqiang Ning, Zhibin Li, Haixiang Cao, Xinhao Wang. Development of chidamide for peripheral T-cell lymphoma, the first orphan drug approved in China. *Intractable & Rare Diseases Research*. **5**(3):185-191(2016).
- [14] MEE-YOUNG AHN. HDAC inhibitor apicidin suppresses murine oral squamous cell carcinoma cell growth in vitro and in vivo via inhibiting HDAC8 expression. *Oncology Letters* **16**: 6552-6560(2018).
- [15] Prasanna P., Joshi T., Pant M., Pundir H., et al. Evaluation of the inhibitory potential of Valproic acid against histone deacetylase of *Leishmania donovani* and computational studies of Valproic acid derivatives. *J. Biomol. Struct. Dyn.*, (2022).
- [16] Almaliti J., Al-Hamashi A. A., Negmeldin A.T., et al. Largazole Analogues Embodying Radical Changes in the Depsipeptide Ring: Development of a More Selective and Highly Potent Analogue. *J. Med. Chem.*, **59**, 10642–10666 (2016).
- [17] Kesharwani S., Sundriyal S., Non-hydroxamate inhibitors of 1-deoxy-D-xylulose 5-phosphate reductoisomerase (DXR): A critical review and future perspective, *Eur. J. Med. Chem.*, **213**, 113055 (2021).
- [18] Alwash AH, Naser NH, Zalzal MH. Design, molecular docking, synthesis, and in vitro pharmacological evaluation of biomolecules-histone deacetylase inhibitors conjugates with carbonylhydrazide as a novel zinc-binding group. *Egypt. J. Chem.*, **65**(10):2-3(2022).
- [19] Benjamin L. Dick and Seth M. Cohen, Metal-Binding Isosteres as New Scaffolds for Metalloenzyme Inhibitors, *Inorg. Chem.*, **57** (15), 9538-9543 (2018).
- [20] Liu Z-Q, Ng Y.M., Tiong P.J., et al, Five-Coordinate Zinc(II) Complex: Synthesis, Characterization, Molecular Structure, and Antibacterial Activities of Bis-[(E)-2-hydroxy-N'-{1-(4-methoxyphenyl)ethylidene}benzohydrazido] dimethylsulfoxidezinc(II) Complex, *Int. J. of Inorg. Chem.*, **2017**,1-8 (2017).
- [21] Hsu1 K.C, Liu C.Y., Lin T.E., Novel Class IIa-Selective Histone Deacetylase Inhibitors Discovered Using an *in Silico* Virtual Screening Approach. *Scientific Reports*, **7**: 3228 (2017).
- [22] Raja A, Shekhar N, Singh H, Prakash A, Medhi B. *In silico* discovery of dual active molecule to restore synaptic wiring against autism spectrum disorder via HDAC2 and H3R inhibition. *PLoS ONE*, **17**(7): e0268139 (2022).
- [23] Ammar D. Elmezayen, Yelekçi Kemal. Structure-based virtual screening for novel potential selective inhibitors of class IIa histone deacetylases for cancer treatment. *Computational Biology and Chemistry*, **92**, 107491(2021).
- [24] Shana V. Stoddard, Kyra Dodson, Kamesha Adams and Davita L. Watkins. *In silico* Design of Novel Histone Deacetylase 4Inhibitors: Design Guidelines for Improved Binding Affinity. *Int. J. Mol. Sci.*, **21**, 219(2020).
- [25] Zinad DS, Mahal A, Salman GA, Shareef OA, Pratama MR. Molecular Docking and DFT Study of Synthesized Oxazine Derivatives. *Egypt. J. Chem.*, **65**(7):2-3(2022).
- [26] Kashyap K., Kakkar R., Exploring structural requirements of isoform selective histone deacetylase inhibitors: a comparative *in silico* study. *J. Biomol. Struct. Dyn.*, (2020).
- [27] Richard A. Friesner, Jay L. Banks, Robert B. Murphy, et al. Glide: A New Approach for Rapid, Accurate Docking and Scoring. 1. Method and Assessment of Docking Accuracy. *J. Med. Chem.* **47**, 1739-1749(2004).
- [28] Sastry G.M., Adzhigirey M., Day T., et al. Protein and ligand preparation: parameters, protocols, and influence on virtual screening enrichments. *J Comput Aided Mol Des.*, (2013).
- [29] Harder E., Damm W., Maple J., OPLS3: a force field providing broad coverage of drug-- like small molecules and proteins. *J. Chem. Theory Comput.*, (2015).
- [30] Bowers K.J., Chow E., Xu H., et al. Scalable Algorithms for Molecular Dynamics Simulations on Commodity Clusters. *IEEE Computer Society*. (2006) November 11-17.
- [31] Raman N., Mitu L. Sakthivel A., Pandi M.S.S., Studies on DNA Cleavage and Antimicrobial Screening of Transition Metal Complexes of 4-Aminoantipyrene Derivatives of N2O2 Type. *J. Iran. Chem. Soc.* **6**, (4), 738-748 (2009).